

ThermoCAPTCHA: Privacy-Preserving Human Verification with Farm-Resistant Traceable Tokens

Shovon Paul

School of Computing & Informatics,
University of Louisiana at Lafayette
Lafayette, Louisiana, USA
shovon.paul1@louisiana.edu

Md Imran Hossen

University of Tennessee at
Chattanooga
Chattanooga, Tennessee, USA
MdImran-Hossen@utc.edu

Xiali Hei

School of Computing & Informatics,
University of Louisiana at Lafayette
Lafayette, Louisiana, USA
xiali.hei@louisiana.edu

Abstract

CAPTCHAs remain a critical defense against automated abuse, yet modern systems suffer from well-known limitations in usability, accessibility, and resistance to increasingly capable bots and low-cost CAPTCHA farms. Behavioral and puzzle-based mechanisms often impose cognitive burdens, collect extensive interaction data, or permit outsourcing to human solvers. In this paper, we present THERMOCAPTCHA, a novel privacy-preserving human verification system that uses real-time thermal imaging to detect live human presence without requiring users to solve challenges. A lightweight YOLOv4-tiny model identifies human heat signatures from a single thermal capture, while cryptographically bound traceable tokens prevent forwarding attacks by CAPTCHA farm workers. Our prototype achieves 96.70% detection accuracy with a 73.60 ms verification latency on a low-powered server. Comprehensive security evaluation—including MITM manipulation, spoofing attempts, adversarial perturbations, and misuse scenarios—shows that ThermoCAPTCHA withstands threats that commonly defeat behavioral CAPTCHAs. A user study with 50 participants, including visually challenged users, demonstrates improved accuracy, faster completion times, and higher perceived usability compared to reCAPTCHA v2.

CCS Concepts

• **Security and privacy** → **Authentication; Web application security; Usability in security and privacy.**

Keywords

CAPTCHA, Thermal Imaging, Privacy-Preserving Authentication, Traceable Tokens, Usability, Adversarial Robustness

1 Introduction

CAPTCHAs serve as a foundational defense against automated abuse on the modern web. From preventing fraudulent account registrations to securing e-commerce checkout flows, CAPTCHAs act as a barrier between legitimate users and increasingly capable automated bots. The original principle behind CAPTCHA design was straightforward: pose a task that is easy for humans but difficult for machines [49]. Yet the rapid evolution of machine learning, large-scale CAPTCHA-solving services, and privacy concerns has fundamentally challenged this premise, exposing long-standing weaknesses in widely deployed systems.

Traditional text- and image-based CAPTCHAs exemplify this erosion. Distorted alphanumeric text, once a strong defense, is now easily defeated by modern deep learning techniques [52]. Image-selection CAPTCHAs—such as identifying traffic lights or

crosswalks—became industry standards, but they too are increasingly vulnerable to automated solvers [10, 24]. These challenges also impose notable usability burdens: visually challenged users often cannot complete image-based puzzles, and cultural differences may hinder correct interpretation of visual content [25]. Performance degradation and increased page latency further undermine user experience [7].

Behavioral CAPTCHAs such as reCAPTCHA v2 and v3 attempt to improve usability by replacing explicit puzzles with passive behavioral analysis. These systems infer user legitimacy from mouse movements, timing signals, device fingerprints, or browser patterns [4]. While they reduce user friction in many cases, they introduce significant privacy concerns [40, 42]. Behavioral profiling enables cross-site tracking, raises regulatory implications, and may inadvertently discriminate against users with motor impairments or atypical interaction patterns [23, 26]. Moreover, machine learning models have begun mimicking human-like interaction traces, narrowing the security gap originally promised by behavioral approaches.

An equally persistent challenge is the rise of CAPTCHA farms—organized human-solver operations offering bulk CAPTCHA solving for a few dollars per thousand tasks [1, 9, 37–39]. Farm workers solve CAPTCHA challenges remotely, return the solution token to the attacker, and enable automated misuse of online services. Because existing CAPTCHA designs do not cryptographically bind verification tokens to a specific client environment, such tokens can be freely forwarded or reused. This weakness severely limits the effectiveness of behavioral and puzzle-based CAPTCHAs and remains a critical gap in the design of modern web defenses.

These limitations collectively raise a central research question: *Can we design a CAPTCHA mechanism that avoids cognitive burden, minimizes privacy risk, resists token forwarding by CAPTCHA farms, and remains accessible to users with visual or auditory impairments?*

This work presents THERMOCAPTCHA, a new direction for CAPTCHA design.

ThermoCAPTCHA eliminates puzzle solving and behavioral profiling by authenticating users through a single real-time thermal image capture. Thermal images encode only coarse heat distributions, rendering them non-identifying and inherently privacy-preserving [31, 43]. This property also mitigates traditional spoofing attacks that exploit printed photos or RGB replay attempts. A lightweight YOLOv4-tiny model analyzes a single thermal frame to determine whether it contains a live human heat signature, enabling a one-click CAPTCHA experience that requires minimal cognitive effort and supports users with vision or hearing impairments.

Beyond user verification, ThermoCAPTCHA integrates a cryptographically enforced token architecture designed to resist CAPTCHA farm outsourcing. Each verification request includes a signed hash of thermal metadata containing a nonce and timestamp, ensuring integrity and freshness. The CAPTCHA server issues a response token encrypted under both a server secret key and the target website’s shared key. The token embeds a session identifier and device fingerprint, allowing the server to reject any token forwarded from an external environment or reused outside its validity window. This binding property—absent from existing CAPTCHA systems—prevents attackers from outsourcing challenges to remote solvers, restoring a key security guarantee.

We implement a complete end-to-end prototype to evaluate ThermoCAPTCHA across effectiveness, security, and usability dimensions. Empirically, ThermoCAPTCHA achieves 96.70% human-detection accuracy with an average verification latency of 73.60 ms on a low-powered server, demonstrating practicality for real-time website integration. Our robustness evaluation spans diverse conditions including varying capture distances, camera angles, lighting environments, and cluttered thermal backgrounds. Security analyses show that ThermoCAPTCHA withstands man-in-the-middle manipulation, replay attempts, tampering with digital signatures, thermal spoofing using heated objects or mannequins, and adversarial perturbation attacks.

To assess real-world usability, we conducted a study with 50 participants, including 20 visually challenged users. ThermoCAPTCHA outperformed reCAPTCHA v2 across all measured dimensions: higher accuracy, significantly lower completion time, and improved perceived ease of use. Notably, visually challenged participants achieved performance comparable to normal users, highlighting the system’s accessibility benefits and its potential to reduce long-standing inequities in CAPTCHA interaction.

Contributions. This paper makes the following contributions:

- **A new CAPTCHA paradigm.** We design THERMOCAPTCHA, the first human-verification system that leverages privacy preserving thermal imaging to eliminate puzzles, cognitive load, and behavioral tracking.
- **Farm-resistant token binding.** We introduce a traceable token mechanism that cryptographically binds a CAPTCHA result to a specific session, device context, and thermal metadata, preventing forwarding attacks that undermine existing systems.
- **Comprehensive real-world evaluation.** Using 286 collected thermal images, we train and deploy a YOLOv4-tiny model achieving 96.70% accuracy with 73.60 ms latency. We further evaluate robustness under angle variation, distance changes, camera tilt, and diverse thermal backgrounds.¹
- **Improved accessibility and usability.** A user study with 50 participants shows that ThermoCAPTCHA offers notably faster verification, higher correctness, and better usability—particularly for visually challenged users—compared to reCAPTCHA v2.

¹Appendix A provides complete replication materials, including dataset, model training scripts, implementation code, and usability questionnaire.

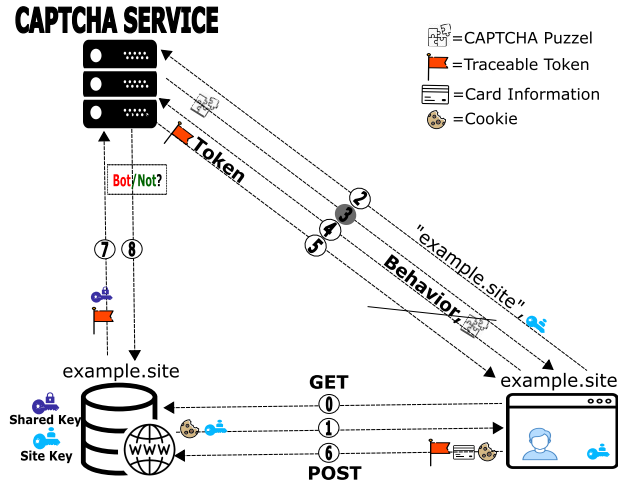


Figure 1: High-level workflow of a modern CAPTCHA [39].

2 Modern CAPTCHAs

Modern CAPTCHA deployments are dominated by behavioral mechanisms introduced by Google in 2013 [4]. Instead of relying exclusively on text distortions or object-recognition puzzles, these systems execute JavaScript in the client’s browser to observe interaction patterns—such as mouse trajectories, timing features, and device artifacts—to distinguish humans from automated bots. Contemporary behavioral CAPTCHAs generally fall into two categories: puzzle-based and puzzle-less.

Puzzle-based CAPTCHAs. Following the shift toward behavioral analysis, puzzle-based CAPTCHAs evolved from static text challenges to interactive visual tasks. Early image-recognition CAPTCHAs, such as Google’s reCAPTCHA, required users to select images containing specific objects, while Arkose Labs offered orientation puzzles and GeeTest introduced slider challenges [44]. reCAPTCHA v2 combined an “I’m not a robot” checkbox with risk scoring derived from user behavior [42]. hCaptcha similarly used image classification tasks and offered dataset-labeling incentives for publishers [2]. Although these systems balance security and usability, they continue to pose accessibility challenges for visually challenged users and often require substantial user interaction [55]. Moreover, visual puzzles remain vulnerable to automated solvers trained on large vision datasets.

Puzzle-less CAPTCHAs. Puzzle-less systems eliminate explicit challenges entirely and rely solely on behavioral signals to determine whether a user is human. reCAPTCHA v2 (in its no-challenge mode), reCAPTCHA v3, and Cloudflare’s Turnstile exemplify this trend [53]. These services compute confidence scores based on browser metadata, device fingerprinting, and user-interaction traces collected during typical page usage, such as form submissions. Although marketed as “CAPTCHA alternatives,” these systems operate within the same verification flow as traditional CAPTCHAs and retain many of the same vulnerabilities—particularly their susceptibility to CAPTCHA farm outsourcing [39].

2.1 Modern CAPTCHA Workflow

Figure 1 summarizes a typical behavioral CAPTCHA workflow. Consider a website `example.site` that deploys a CAPTCHA to protect a high-value action such as concert ticket purchases. The site embeds provider-supplied JavaScript—including a *site-key* that identifies the domain—which initializes CAPTCHA collection upon page load. Providers discourage deferred or lazy loading because early execution maximizes behavioral-signal fidelity [5]. The website and CAPTCHA provider share a *shared-key* for secure server-to-server verification.

When a user visits `example.site`, their browser sets a cookie ① and loads the CAPTCHA script ①. The script queries the CAPTCHA provider with the *site-key* ②. Since Referer headers may be suppressed by users or browsers, the *site-key* serves as the reliable identifier for the requesting website. The provider may return an explicit puzzle ③, though puzzle-less systems omit this step. Once the puzzle is solved—or upon a relevant browser event in puzzle-less systems—the client transmits behavioral features and optional puzzle solutions back to the provider ④. The provider generates a *token* encoding a risk score and returns it to the client site ⑤.

The website attaches this token to sensitive form data, such as payment information, and forwards it to its server ⑥. The server validates the token by contacting the CAPTCHA provider with the token and the site’s secret *shared-key* ⑦. Tokens are time-limited (e.g., two minutes for reCAPTCHA) and must be validated promptly to prevent reuse [39]. The provider computes a final risk decision ⑧, which site developers interpret according to their security requirements.

2.2 CAPTCHA Farms

Despite advances in behavioral modeling, modern CAPTCHAs remain vulnerable to CAPTCHA farm outsourcing [39]. These human-solver markets have operated for more than a decade, allowing attackers to relay CAPTCHA challenges to low-wage workers who solve them manually. Motoyama et al. [37] documented the economic structure of such farms, which typically consist of (1) an attacker-facing API through which CAPTCHA images or tokens are submitted, and (2) a worker interface that streams challenges to human solvers using lightweight desktop or browser tools.

This model persists today. Services such as Anti-Captcha and Kolotibablo continue to support new behavioral CAPTCHA formats and maintain stable pricing between \$1 and \$4 per thousand solves [14, 17, 29, 41]. Crucially, behavioral CAPTCHAs provide no mechanism to bind a verification token to the client environment that generated it. As a result, attackers can submit a CAPTCHA challenge from an automated system, relay it to a remote worker, and attach the returned token to their malicious workflow—effectively bypassing behavioral analysis and rendering puzzle complexity irrelevant. This persistent vulnerability underscores the need for CAPTCHAs that enforce cryptographic, context-sensitive token binding.

3 Threat Model

ThermoCAPTCHA operates within the standard web-security model used by existing CAPTCHA systems such as reCAPTCHA. Our

threat model focuses on adversaries attempting to bypass human verification, impersonate users, manipulate thermal captures, or exploit weak token-binding mechanisms. We outline the assumptions and security boundaries below.

Client-Side Script Integrity and Webcam Access. We assume that browsers correctly retrieve and execute ThermoCAPTCHA’s JavaScript from the CAPTCHA server when the protected webpage loads. To ensure integrity, the script is delivered with Subresource Integrity (SRI) metadata; any modification to the script causes the browser to reject execution. The browser’s native permission model governs thermal-camera access, and a thermal capture is performed only when the CAPTCHA component is triggered, with the video stream terminating immediately afterward. *We further assume that adversaries may attempt to present fabricated or manipulated thermal inputs—such as heated objects, replayed captures, or adversarially perturbed images—with the goal of deceiving the human-detection model. ThermoCAPTCHA must therefore be robust against such spoofing attempts.*

Server-Side Security. We assume a hardened and uncompromised CAPTCHA backend server. The server stores sensitive material such as nonces, session identifiers, and secret keys—encrypted at rest using AES-256 and transmits all data exclusively over secure channels (TLS 1.2 or higher). Strong access control, multi-factor authentication for administrative interfaces, periodic penetration testing, and routine key rotation are in place. The server maintains data integrity using cryptographic hash functions and enforces strict validation on all incoming client metadata and thermal-image signatures.

Website–CAPTCHA Server Synchronization. The protected website and the ThermoCAPTCHA server communicate through a pre-established *shared-key*. We assume that both parties follow secure key-management practices, including regular key rotation and protection of keys at rest. Synchronization mechanisms ensure consistent timing windows for validating signed thermal metadata (e.g., timestamps, nonces), preventing acceptance of stale or replayed verification attempts. Misalignment between server and website clocks, when it occurs, is assumed to be small and bounded.

User Privacy Requirements. Thermal captures used by ThermoCAPTCHA contain coarse heat-distribution patterns that cannot uniquely identify individuals [15, 31, 43]. Nonetheless, we assume that the service adheres to strong privacy-preserving data-handling practices. Thermal images are anonymized, encrypted at rest, and accessible only to authorized personnel under multi-factor authentication. Retention is minimized: images are stored only for the brief period needed for verification, after which they are securely deleted. These safeguards mitigate privacy risks even in the event of partial system compromise.

4 ThermoCAPTCHA System

Our goal is to design a real-world, image-based CAPTCHA that (i) protects user privacy, (ii) resists outsourcing to CAPTCHA farms, and (iii) preserves the low-friction experience of one-click behavioral CAPTCHAs. ThermoCAPTCHA achieves this by combining privacy-preserving thermal imaging with cryptographically bound,

farm-resistant tokens, while remaining compatible with standard web architectures.

We distilled our design into three guiding goals:

- **Service-agnostic deployment.** ThermoCAPTCHA should integrate into existing web infrastructures using the same client-server pattern as systems like reCAPTCHA, without requiring application-specific changes or trusted hardware, and while minimizing the attack surface exploited by CAPTCHA farms [39].
- **Fast, web-scale operation.** Verification must complete within tens of milliseconds on commodity servers to be viable for high-traffic sites and latency-sensitive user flows.
- **Privacy and ethical robustness.** The system should avoid identity linkage, behavioral profiling, and continuous video capture, especially given the ethical risks of camera-based detection systems [30].

4.1 System Design

ThermoCAPTCHA is designed as a drop-in replacement for traditional behavioral CAPTCHAs. As in reCAPTCHA-style deployments, the protected website embeds a provider-hosted JavaScript widget and uses a *site-key* and *shared key* to communicate with the CAPTCHA service. Rather than collecting mouse trajectories or displaying puzzles, the widget performs a single thermal image capture when the protected action is triggered (e.g., form submission or checkout), then offloads verification to the ThermoCAPTCHA server.

We initially considered alternative signals such as RGB webcam images or keystroke/mouse dynamics to support users with visual and auditory impairments. However, RGB images and behavioral traces raise significant privacy risks: they enable biometric identification, cross-site behavioral profiling, and long-term tracking even if transported over encrypted channels. These properties conflict with our goal of minimizing data sensitivity and ethical risk. As a result, we discarded these designs in favor of thermal imaging.

Thermal imaging as a privacy-preserving signal. Thermal cameras have lower spatial resolution than typical visible-light cameras and primarily encode heat distribution rather than detailed texture. Prior work shows that thermal images alone do not support reliable, fine-grained identification of individuals, especially under realistic variations such as masks, glasses, and changing ambient temperature conditions [15, 27, 31, 43]. External factors (e.g., activity level, emotional state, environment) further distort thermal signatures, making them unsuitable for robust biometric recognition.

These properties make thermal images attractive for a *user-agnostic* CAPTCHA: ThermoCAPTCHA only needs to recognize that a live human is present, not *which* human. Thermal frames therefore provide a coarse but sufficient signal for liveness and human presence, without exposing unique identity features. However, thermal captures are still data objects that can be intercepted and replayed; protecting them against man-in-the-middle (MITM) attacks requires additional cryptographic mechanisms.

Digital signatures on thermal captures. To defend against replay and in-transit manipulation of thermal captures, ThermoCAPTCHA signs the hash of each captured image plus freshness metadata,

rather than encrypting the image itself. We considered two approaches: (i) encrypting the thermal image with AES-256 and then signing its SHA256 hash with RSA, or (ii) directly signing the SHA256 hash of the image and metadata using RSA signatures [12, 34]. Because thermal frames are already privacy-preserving and do not contain unique identity features, confidentiality is not strictly required. We therefore adopt the second approach for lower computational overhead and simpler integration with existing web stacks.

Concretely, when a user triggers ThermoCAPTCHA, the client widget:

- (1) Captures a thermal frame and converts it to a binary representation.
- (2) Appends a freshly generated nonce and timestamp to the image metadata, yielding a *binary-with-metadata* object.²
- (3) Computes a SHA256 hash of this object and signs it with the user’s private key using RSA³ to produce a digital signature.
- (4) Sends a payload containing the domain name, user IP, *site-key*, *binary-with-metadata* object, digital signature, and the user’s public key to the ThermoCAPTCHA server (Figure 2(b)).

Upon receipt, the server reconstructs the hash of the *binary-with-metadata* object and verifies the signature using the provided public key. Because the hash covers the image data, nonce, and timestamp, any modification to the image (or associated metadata) causes verification to fail. The server also enforces a tight time window (two minutes in our implementation) and rejects reused nonces to prevent replay of old captures. This combination of hashing and digital signatures ensures integrity, authenticity, and freshness of the submitted thermal frames.

Farm-resistant traceable tokens. CAPTCHA farms routinely break behavioral systems by solving challenges on their own infrastructure and returning tokens to attackers via APIs (e.g., Anti-Captcha, Kolotibablo) [14, 17, 29, 39, 41]. Through MITM analysis using tools like *mitmproxy* [35], we observe that these services forward site-specific metadata (such as the *site-key* and URL) to workers, who use browser extensions or automated browsers to simulate visits and obtain valid tokens. Because existing CAPTCHA tokens are not bound to a particular device or session context, attackers can reuse them in arbitrary environments.

ThermoCAPTCHA addresses this by issuing *traceable tokens* that are cryptographically bound to the originating user session and device. For each completed thermal verification, the server generates a unique *sessionID* and device *fingerprint* and stores them in a session table. It then constructs a payload containing the user identifier, *sessionID*, *fingerprint*, nonce, and expiration timestamp, signs it as a JSON Web Token (JWT), and encrypts it using Fernet with both the CAPTCHA server’s secret key and the website’s shared key.⁴ The resulting ciphertext is returned to the client website as the ThermoCAPTCHA token.

When the protected website later presents this token for final verification, the ThermoCAPTCHA server decrypts it, re-checks the nonce and timestamp, and verifies that the embedded *sessionID* and

²Adding a nonce and timestamp to the image metadata increases the binary size by 72 bytes without affecting human detection.

³We chose RSA over ECC due to its widespread deployment and compatibility with existing infrastructures.

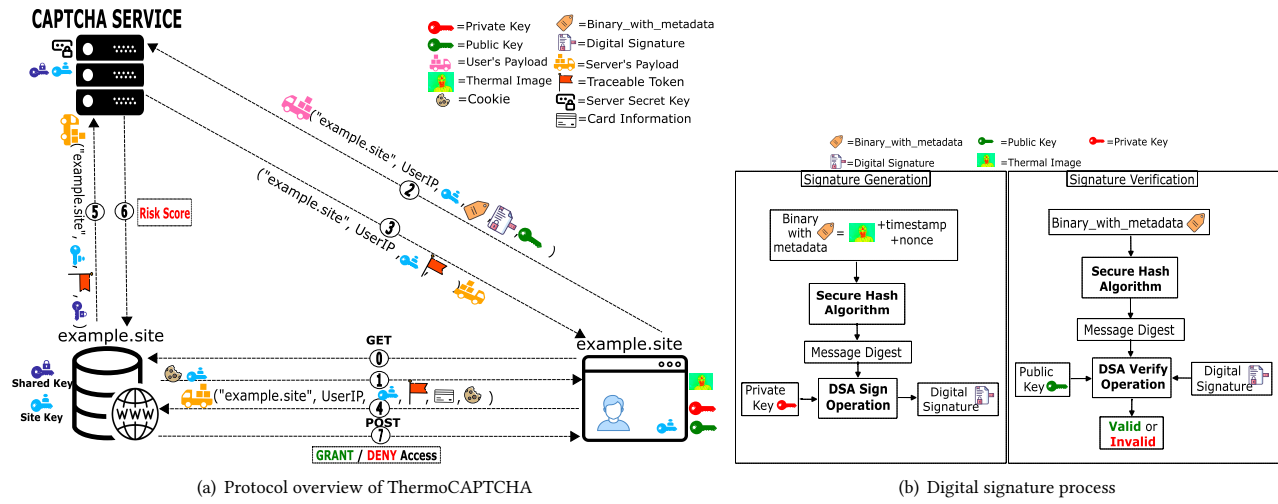


Figure 2: ThermoCAPTCHA system overview.

fingerprint match an active session record. Any discrepancy (e.g., a token replayed from a different device or network) causes verification to fail. As a result, tokens obtained by CAPTCHA farm workers cannot be forwarded or reused outside their original context.

4.2 Protocol Overview

Figure 2(a) illustrates ThermoCAPTCHA’s high-level protocol, which mirrors the flow of modern behavioral CAPTCHAs (Figure 1) while replacing behavioral signals with thermal captures and traceable tokens.

At a high level, the workflow proceeds as follows (see also Figure 3):

- Initialization (user → website).** When a user visits a protected section of `example.site` (e.g., ticket purchase), the website sets a cookie, loads the ThermoCAPTCHA script with its `site-key`, and prepares to gate the critical action on CAPTCHA verification.
- Thermal capture and signed submission (user → ThermoCAPTCHA).** Upon trigger (e.g., form submission), the client widget captures a thermal image, embeds a nonce and timestamp into its metadata, computes a hash, signs it with the user’s private key, and sends the resulting payload (including the binary-with-metadata, signature, and public key) to the ThermoCAPTCHA server.
- Verification and token issuance (ThermoCAPTCHA → user).** The server validates that the payload contains a valid thermal image, enforces nonce uniqueness and timestamp freshness, and verifies the digital signature. It then runs the YOLOv4-tiny model (Section 5) to compute a human-detection confidence score, stores this score in its database, and issues a traceable token bound to the corresponding user/session/device context. The token is returned to the client website.
- Final token validation (website ↔ ThermoCAPTCHA).** The website attaches the ThermoCAPTCHA token to its

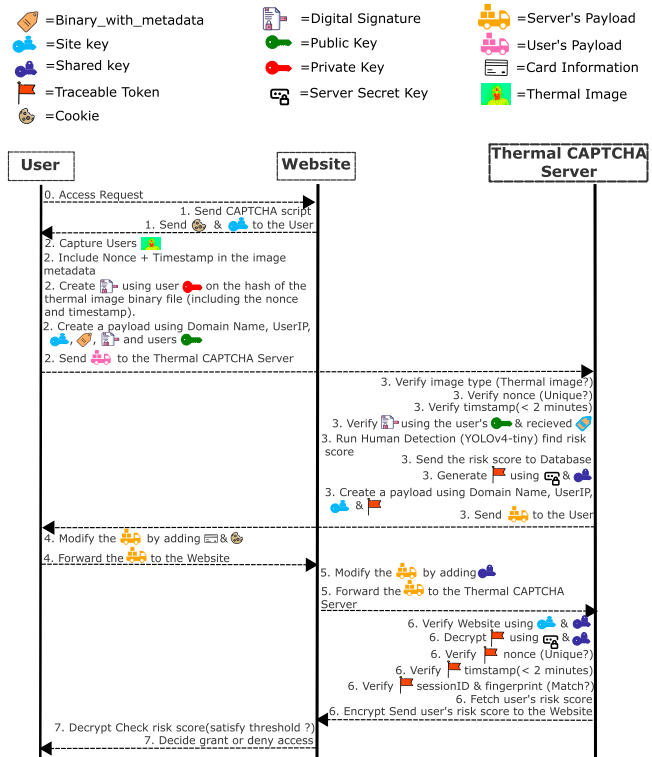


Figure 3: Workflow of the ThermoCAPTCHA system.

application-level request (e.g., payment information) and forwards it, along with its shared key, to the ThermoCAPTCHA server for verification. The server checks the site-key/shared-key pair, decrypts and validates the token (including nonce, timestamp, sessionID, and fingerprint), and retrieves the stored risk score.

- Decision (website → user).** ThermoCAPTCHA returns the encrypted risk score to the website, which decrypts it and applies local policy (e.g., thresholding) to accept or

⁴We use Fernet for ease of integration with Python; JSON Web Encryption (JWE) could be used equivalently.

reject the action. The final allow/deny decision remains under the website’s control.

This design preserves the deployment model of existing CAPTCHA services while introducing two key changes: (1) verification is based on a single thermal frame processed by a compact detector, and (2) tokens are cryptographically bound to the originating execution context, preventing CAPTCHA-farm relaying without requiring changes to the web application’s control flow.

5 Human-Detection Model (YOLOv4-tiny)

ThermoCAPTCHA relies on a lightweight object detector to decide whether a submitted thermal frame contains a live human. In this section, we describe the YOLOv4-tiny-based model used for this task, along with our preprocessing and training procedure.

Network architecture. Our detector is based on the YOLOv4-tiny architecture, chosen for its favorable trade-off between accuracy and inference speed on commodity hardware. YOLOv4-tiny is a compressed variant of YOLOv4 with substantially fewer parameters and layers (29 convolutional layers and two YOLO detection heads, compared to 137 layers in the full model), enabling real-time operation on non-GPU servers. Although slightly less accurate than full YOLOv4, YOLOv4-tiny is reported to be up to eight times faster on the MS COCO benchmark [3], which aligns with our requirement to keep CAPTCHA verification latency in the tens-of-milliseconds range.

We adapt YOLOv4-tiny for binary human-presence detection in thermal images. Specifically, we configure the network as a single-class detector and adjust the convolutional filters in the layers immediately preceding each [yolo] detection head using the standard formula $\text{filters} = (\text{classes} + 5) * 3$ (for three anchor masks), setting $\text{classes} = 1$. The resulting model predicts bounding boxes corresponding to human heat signatures; ThermoCAPTCHA then reduces this to a binary decision (human present / not present) based on the detector outputs.

Image preprocessing and augmentation. To improve generalization from a relatively small custom dataset, we apply standard data-augmentation techniques tailored to our setting. Our base dataset consists of 286 thermal images collected from 26 participants (details in Appendix C). From these, we randomly select 176 images and generate 20 augmented variants per image using random geometric and photometric transformations. Following the taxonomy of Shorten and Khoshgoftaar [46], we apply random rotation, translation, shear, zoom, and horizontal flipping, as well as brightness and scale adjustments.

Concretely, we set $\text{rotation_range} = 40$, $\text{horizontal_flip} = \text{True}$, $\text{height_shift_range} = 0.2$, $\text{shear_range} = 0.2$, $\text{zoom} = 0.2$, $\text{width_shift_range} = 0.2$, and $\text{fill_mode} = \text{'nearest'}$. This process yields 3,520 augmented thermal images in total, exceeding the YOLOv4 guideline of at least 2,000 images for effective single-class training [3]. All images are resized to 416×416 pixels and normalized before being fed to the network.

Training procedure. We partition the augmented dataset into training, validation, and test splits to enable principled hyperparameter tuning and unbiased evaluation. Using the validation set,

we perform manual hyperparameter search and obtain the following configuration: batch size of 64, input resolution 416×416 , momentum 0.9, weight decay 0.0005, saturation factor 1.5, exposure factor 1.5, and jitter 0.3, with an initial learning rate of 0.00261. The loss function and optimization procedure follow the standard YOLOv4-tiny training setup.

Training is run for 40,000 iterations, after which the model reaches an average loss of 0.0509, consistent with the range typically observed for well-converged YOLOv4-tiny detectors. We evaluate several candidate checkpoints on the held-out test set and perform a comparative analysis of the resulting weights (Appendix C, Table 10). The model corresponding to `yolov4-custom_30000.weights` achieves the best mean average precision (mAP) and an overall human-detection accuracy of **96.70%**, and is therefore selected as the deployed detector in ThermoCAPTCHA.

6 Experimental Setup

6.1 Camera Setup

To implement and evaluate ThermoCAPTCHA, we constructed two thermal-imaging module configurations. The first configuration, used for dataset collection and model training, employs an OpenMV Cam H7 R2 microcontroller paired with a FLIR® Lepton® Adapter Module and a Teledyne FLIR Lepton 500-0771-01 thermal sensor. This combination provides high-resolution thermal frames suitable for training the YOLOv4-tiny detector.

For real-time CAPTCHA verification, we built a second configuration using the PureThermal 2 FLIR Lepton Smart I/O Module equipped with the same Lepton 500-0771-01 sensor. PureThermal 2 was chosen for its plug-and-play installation and native UVC compatibility, enabling seamless deployment as a thermal webcam on commodity operating systems. The assembled thermal module used in our prototype is shown in Figure 7 (Appendix B).⁵

6.2 Data Collection

Because no suitable public dataset of human thermal images exists for CAPTCHA-style liveness verification, we created a custom dataset specifically for this study. The dataset contains 286 thermal images collected from 26 participants. Each participant contributed 11 images: nine captured at 10-degree increments along the x-axis between 50° and 130° , and two additional images captured at a fixed 90° orientation with a $\pm 10^\circ$ tilt on the y-axis. This procedure ensures diversity in facial orientation and head pose, which is critical for training a robust human-presence detector.

The full experimental environment used during image collection is described in Appendix B, and additional dataset statistics and augmentation details appear in Appendix C.

7 Evaluation

We now evaluate proposed ThermoCAPTCHA along several dimensions. Our study is guided by the following research questions:

- **RQ1 – System Effectiveness.** How accurately and efficiently does ThermoCAPTCHA detect human presence

⁵Our complete plug-and-play module can be reproduced using parts from <https://www.sparkfun.com/products/20813>.

Table 1: Baseline effectiveness of the ThermoCAPTCHA under controlled conditions (3 ft distance, frontal position).

Metric	Value
Accuracy	96.70%
Images evaluated	120
Correct detections	116
Average latency	73.60 ms
Server hardware	i5-8550U, 8 GB RAM, MX150 GPU

under realistic deployment conditions (e.g., varying angles, distances, and background environments)?

- **RQ2 – Security Against Adversaries.** To what extent does the proposed system withstand practical attacks, including man-in-the-middle manipulation, spoofing attempts, adversarial perturbations, and cross-entity token reuse by CAPTCHA farms?
- **RQ3 – Robustness to Real-World Misuse and Input Manipulation.** Can the system be bypassed using non-thermal images, compromised client-side execution (e.g., absence of SRI), or physical thermal forgeries such as heated objects or mannequins?

Unless otherwise stated, all experiments use the YOLOv4-tiny model described in Section 5. All evaluations are conducted exclusively on thermal samples not used during training or validation. For consistency across experiments, a detection is considered correct if the model’s confidence score exceeds 0.50.

7.1 RQ1 – System Effectiveness

RQ1 evaluates the practical viability of the ThermoCAPTCHA by measuring its ability to (1) reliably detect human presence under realistic deployment conditions, and (2) respond within latency constraints consistent with modern, interactive CAPTCHA systems.

7.1.1 Detection Accuracy and Latency in Controlled Conditions. We deployed ThermoCAPTCHA on a live website backed by a Flask API and an SQLite3 database, running on a low-power Ubuntu 20.04 server equipped with an Intel Core i5-8550U CPU, 8 GB RAM, and an NVIDIA MX150 GPU. In a controlled environment (73°F, user distance of 3 ft), the system correctly identified 116 of 120 thermal images, yielding an accuracy of **96.70%**. The end-to-end verification latency—measured from image submission to risk-score generation—averaged **73.60 ms**, well within the responsiveness expected of modern CAPTCHA mechanisms. Table 1 summarizes the baseline performance metrics.

7.1.2 Impact of Viewing Angle and Camera Tilt. We next examine robustness to natural variations in user posture and webcam placement. Participants were recorded at horizontal angles from 50° to 130° in 10° increments, with 90° serving as the frontal reference. As shown in Table 2, detector confidence peaks at 90° (0.91 ± 0.070) and declines toward oblique angles, reaching 0.79 ± 0.118 at 130°. This degradation aligns with reduced visibility of the head and torso heat signature at extreme viewpoints.

We additionally varied the vertical tilt between 80°, 90°, and 100°. Table 2 shows a modest improvement at 100° (0.92 ± 0.070), which

Table 2: YOLOv4-tiny confidence across horizontal and tilt angles. Values reported on a 0–1 confidence scale.

Angle Type (°)	Samples (n)	Mean Conf.	Std. Dev.
Horizontal Viewing Angles			
50	10	0.82	0.095
60	10	0.85	0.088
70	10	0.88	0.080
80	10	0.90	0.072
90	10	0.91	0.070
100	10	0.89	0.078
110	10	0.86	0.090
120	10	0.83	0.102
130	10	0.79	0.118
Tilt Angles			
80	10	0.87	0.085
90	10	0.89	0.078
100	10	0.92	0.070

Table 3: YOLOv4-tiny detection confidence at varying user-camera distances. Values reported on a 0–1 confidence scale.

Distance (ft)	Samples (n)	Mean Conf.	Std. Dev.
3	27	0.91	0.042
4	27	0.88	0.055
5	27	0.84	0.061
6	27	0.80	0.073

we attribute to more direct exposure of the upper-body thermal region. These findings indicate that the system tolerates ordinary positional variation without meaningful performance loss.

7.1.3 Impact of User Distance. To quantify the effect of user-camera separation, nine participants captured thermal images at distances of 3 ft, 4 ft, 5 ft, and 6 ft. Each participant provided three images per distance, yielding **27 samples per distance**. Table 3 shows a gradual, monotonic decline in detector confidence as distance increases, driven primarily by reduced thermal resolution and lower pixel density on facial features at longer ranges. Confidence remains high at 3 ft (0.91 ± 0.042) and decreases to 0.80 ± 0.073 at 6 ft.

Despite this reduction in confidence, the detector correctly classified all samples as human across every distance tested. This result demonstrates that human heat signatures remain reliably distinguishable even near the operational limits of compact consumer-grade thermal sensors.

7.1.4 Robustness to Background Variation. To approximate real-world deployment, nine participants captured three thermal images each in uncontrolled home environments, yielding **27 samples per background condition**. Environments included direct sunlight, heat-emitting appliances, low-light rooms, distant subject placement, and scenarios involving significant body rotation. Representative thermal samples from these settings are shown in Figure 4.

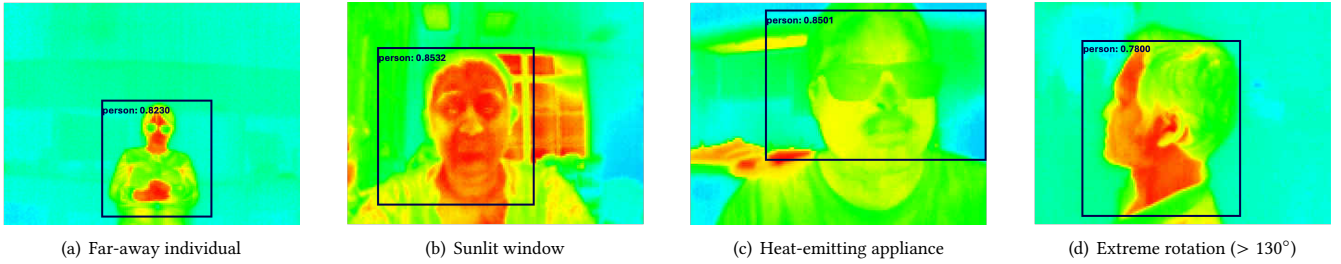


Figure 4: Thermal samples collected under diverse background conditions, including distant subjects, direct sunlight, heat-emitting objects, and extreme body rotation.

Table 4: Detection confidence across diverse background conditions. Each condition includes 27 thermal captures.

Background Condition	Samples (n)	Mean Conf.	Std Dev.
Sunlit window	27	0.89	0.058
Heat-emitting object	27	0.87	0.062
Low-light room	27	0.90	0.049
Distant subject	27	0.82	0.071
Extreme rotation	27	0.80	0.075

Table 4 reports the corresponding detector confidence scores. Human detection confidence remains high (0.87–0.90) across conditions such as sunlit windows, low-light rooms, and household heat sources. More challenging configurations—distant subjects (0.82 ± 0.071) and extreme rotation (0.80 ± 0.075)—exhibit moderate reductions in confidence, as expected from diminished visibility of core thermal features. Importantly, the detector correctly classified *all* samples as human, demonstrating resilience to thermal clutter and environmental variation commonly encountered in home and office settings.

RQ1 Findings. ThermoCAPTCHA achieves high accuracy and low verification latency under controlled conditions, while maintaining robustness to variations in user posture, camera angle, distance, and background environments. Confidence declines predictably with user–camera distance due to sensor resolution limits, but all human samples were successfully detected across all tested scenarios. These results demonstrate that the system performs reliably under realistic deployment conditions.

7.2 RQ2 – Security Against Adversaries

RQ2 examines whether ThermoCAPTCHA design withstands practical attacks from network adversaries, spoofing adversaries, and machine-learning–based adversaries. We evaluate resilience against (1) man-in-the-middle (MITM) manipulation, (2) token forwarding and reuse by CAPTCHA farm workers, (3) physical and thermal spoofing, and (4) adversarial perturbations targeting the human-detection model.

Adversary Model. We consider three classes of adversaries: (1) a network adversary capable of observing, replaying, or modifying messages; (2) an application-layer adversary who attempts to reuse tokens obtained through CAPTCHA-farm outsourcing; and (3) a computational adversary who crafts spoofed or adversarial inputs

Table 5: MITM attack outcomes across 2,500 adversarial attempts.

Attack Type	Attempts	Accepted	Rejected	Success (%)
Replay	500	0	500	0.0
Stale timestamp	500	0	500	0.0
Nonce reuse	500	0	500	0.0
Modified binary	500	0	500	0.0
Modified metadata	500	0	500	0.0

to the detection model. The adversary does not compromise the CAPTCHA server, which is consistent with the trust assumptions of modern behavioral CAPTCHA deployments.

7.2.1 Resistance to Man-in-the-Middle Manipulation. We first considered adversaries capable of intercepting, modifying, or replaying messages exchanged between the client, web server, and CAPTCHA server. Using *mitmproxy*, we conducted five classes of MITM attacks: (1) replay of valid payloads, (2) submission of stale timestamps, (3) nonce reuse, (4) binary-level tampering, and (5) metadata-only tampering. Each attack class was executed 500 times, yielding a total of 2,500 adversarial requests.

Table 5 reports that *all* adversarial attempts were rejected, producing a 0% success rate across all categories. Replay and stale-timestamp attacks failed due to freshness checks, nonce reuse was blocked by server-side uniqueness validation, and any modification to the binary or metadata invalidated the digital signature.

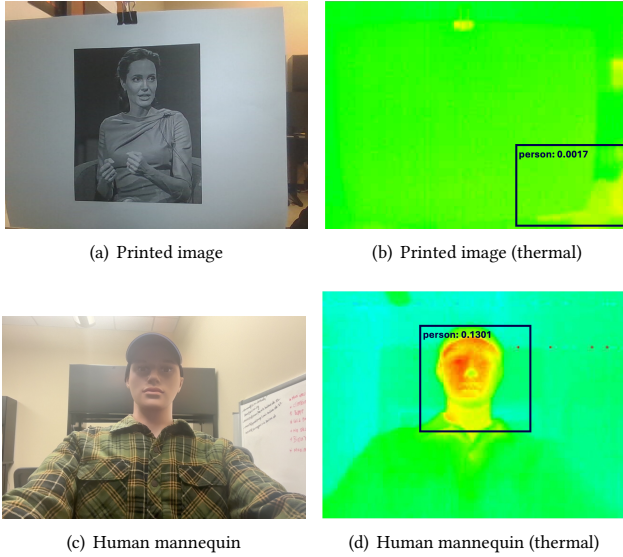
The only meaningful threat remaining is a full server compromise, which lies outside our trust model and is similarly catastrophic for today’s major CAPTCHA deployments (e.g., reCAPTCHA, h-Captcha). These results support that the protocol enforces end-to-end integrity and freshness properties consistent with standard cryptographic practice, while covering the full MITM attack surface considered in prior CAPTCHA and web security studies.

7.2.2 Resistance to CAPTCHA-Farm Token Reuse. A common evasion strategy for behavioral CAPTCHAs is to outsource challenges to human solvers in CAPTCHA farms. We therefore evaluate whether a valid traceable token generated for a worker W can later be reused by an attacker A operating under a different device fingerprint, session identifier, and IP context.

We simulated farm-style outsourcing with $N \in \{100, 500, 1000\}$ valid tokens obtained by W . For each token, the attacker attempted exactly one reuse from a separate device configuration, yielding

Table 6: Traceable-token reuse outcomes across 1,600 adversarial attempts.

N Tokens	Attempts	Accepted	Rejected	Success (%)
100	100	0	100	0.0
500	500	0	500	0.0
1000	1000	0	1000	0.0

**Figure 5: Printed human image and heated mannequin compared with their thermal counterparts. Neither spoofed input was classified as human.**

1,600 total reuse attempts. Table 6 shows that none of the reuse attempts succeeded.

These results demonstrate that forwarding a traceable token is ineffective: the dual-key-encrypted token is cryptographically bound to the originating `sessionId`, device fingerprint, nonce, and expiration timestamp, and thus cannot be validated in any foreign execution context. This empirical finding is consistent with our formal analysis in Appendix E, which shows that any replay attempt by an attacker A fails the MAC verification whenever the tuple $(UID, sess_{id}, dev_{fp}, nonce, exp)$ differs from that of the original solver W .

In contrast to behavioral CAPTCHAs such as reCAPTCHA and hCaptcha—which have no mechanism to bind a token to a particular client—our design introduces a cryptographically enforced, per-session binding that prevents the economic outsourcing attack fundamental to CAPTCHA-farm operations.

7.2.3 Resistance to Physical and Thermal Spoofing. We next evaluate whether attackers can fool the system using printed photos, thermal forgeries, or objects heated to human-like temperatures. Printed faces (Figure 5) produced no visible features in thermal space, preventing the model from generating bounding boxes or confidence scores. Heating a human mannequin with a heat gun yielded diffuse and unrealistic thermal gradients, which YOLOv4-tiny did not classify as human.

Table 7: Summary of FGSM adversarial outcomes across 20 samples.

ϵ	Misclassifications	Success (%)
0.01–0.10	0/20	0%
0.20	1/20	5%
0.30	6/20	30%
0.50	16/20	80%

These results indicate that reproducing the tight, high-gradient thermal patterns of a real human body using inanimate objects is difficult in practice, providing an inherent layer of physical liveness protection absent from standard RGB-based CAPTCHAs.

7.2.4 Resistance to Adversarial Perturbations (FGSM). Finally, to evaluate vulnerability to ML-driven evasion, we applied FGSM perturbations to 20 thermal samples (10 human, 10 non-human) using $\epsilon \in \{0.01, 0.02, 0.03, 0.10, 0.20, 0.30, 0.50\}$. A concise summary of attack outcomes is shown in Table 7. The complete, per-class breakdown appears in Appendix D.

These results show that perturbations up to $\epsilon \leq 0.10$ produce no errors, indicating strong intrinsic robustness of thermal patterns. Higher-magnitude perturbations ($\epsilon \geq 0.30$) cause failures but also introduce visually unrealistic artifacts that are infeasible to produce during live thermal capture. Detailed evasion/induction results are provided in Appendix D.

RQ2 Findings. The ThermoCAPTCHA withstands practical network, spoofing, and ML-driven attacks. MITM manipulation and token forwarding were entirely unsuccessful across thousands of adversarial attempts. Physical spoofing attempts failed due to the unique thermal characteristics of the human body, while FGSM perturbations only succeed under unrealistically large distortion budgets. These results demonstrate that the proposed design provides strong protection against adversaries that routinely defeat conventional behavioral CAPTCHAs.

7.3 RQ3 – Robustness to Real-World Misuse and Input Manipulation

RQ3 evaluates whether the ThermoCAPTCHA fails safely under deployment mistakes, malformed inputs, or benign but atypical usage conditions. Unlike RQ2—which considers deliberate adversarial manipulation—RQ3 focuses on input conditions that arise unintentionally in practice. We study three common categories of misuse: (1) non-thermal or improperly encoded uploads, (2) submissions originating from compromised clients lacking Subresource Integrity (SRI), and (3) genuine thermal images that contain non-human heat sources. The non-thermal evaluation includes 80 samples across four image categories (20 each), while the compromised-client and non-human thermal evaluations each use 40 and 80 samples, respectively.

7.3.1 Handling Non-Thermal Inputs and Encoding Misuse. To assess robustness against incorrectly formatted inputs, we submitted 80

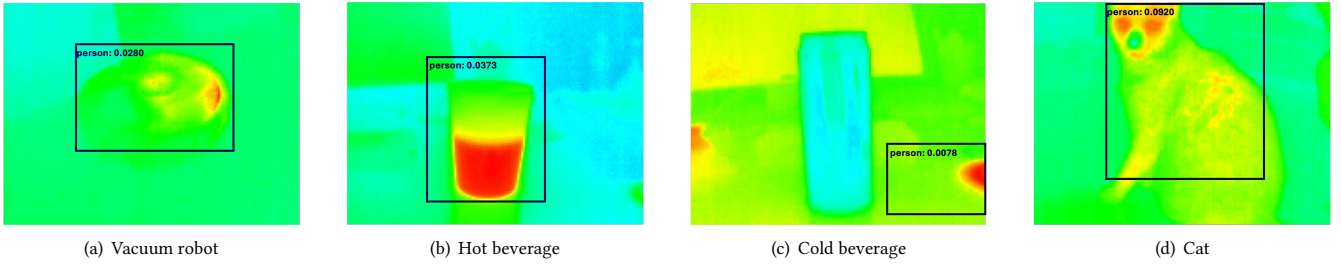


Figure 6: Examples of non-human thermal sources used to evaluate robustness to misuse and incidental hot objects. None of these inputs was detected as human.

non-thermal images to the CAPTCHA endpoint, consisting of 20 RGB photographs, 20 grayscale images, 20 synthetic images, and 20 desktop screenshots. Although these submissions preserved the expected request structure, none complied with the thermal encoding required by the server.

Across all 80 submissions, the system rejected the input during the initial format- and metadata-validation phase, resulting in a rejection rate of **100%**. No malformed input propagated to the YOLOv4-tiny detector. This quantitatively demonstrates that ThermoCAPTCHA enforces strict type and encoding checks, ensuring that deployment errors or client misuse fail safely and cannot be exploited as unintended authentication pathways.

7.3.2 Execution Under Compromised or Non-SRI Client Environments. To evaluate exposure to client-side compromise, we simulated a browser environment without SRI enforcement. An attacker-controlled script submitted 40 manipulated payloads: 20 recompressed or modified thermal images and 20 metadata-tampered submissions (e.g., altered timestamps, missing fields, or invalid signatures).

All 40 submissions were rejected during digital-signature validation or nonce verification, resulting in a **0% acceptance rate**. Even minor re-encoding of thermal frames caused signature mismatch, indicating that the security of the ThermoCAPTCHA does not depend on client-side integrity controls such as SRI.

7.3.3 Non-Human Thermal Sources and Incidental Hot Objects. To assess robustness against benign but atypical thermal inputs, we evaluated 80 genuine thermal images that did not contain human subjects. These consisted of 20 vacuum robot captures, 20 hot objects (e.g., a recently boiled cup), 20 cold objects, and 20 pet/animal samples. All inputs follow the correct thermal encoding and therefore represent realistic misuse scenarios rather than malformed data.

Table 8 reports the corresponding detection outcomes. Across all 80 samples, the detector produced either no bounding box or extremely low confidence scores (< 0.10), yielding a **0% false-acceptance rate**. These results indicate that non-human heat signatures—even when warm, structured, or visually similar to a human silhouette—do not mimic the spatial and geometric thermal patterns that the detector associates with human presence.

Table 8: Detection outcomes for non-human thermal sources (80 samples total).

Input Type	Samples	False Accepts	FAR (%)
Vacuum robot	20	0	0.0
Hot object	20	0	0.0
Cold object	20	0	0.0
Pet/animal	20	0	0.0
Total	80	0	0.0

Representative examples are shown in Figure 6. These results demonstrate that incidental heat sources do not trigger false positives, and that the system preserves safety even when users unintentionally capture warm objects, household devices, or pets during CAPTCHA interaction.

RQ3 Findings. The ThermoCAPTCHA fails safely under realistic deployment mistakes and benign misuse. All non-thermal images were rejected prior to model invocation, all manipulated submissions from compromised clients failed signature and freshness checks, and none of the non-human thermal sources were misclassified as humans. These results complement the adversarial robustness demonstrated in RQ2 and show that the system maintains strong safety and correctness guarantees under real-world operating conditions.

8 User Study Methodology

To assess usability and accessibility, we conducted a comparative user study of THERMOCAPTCHA and Google reCAPTCHA. The study measured (1) task completion time, (2) correctness, and (3) subjective user experience. reCAPTCHA was integrated into our lab homepage using the public API, while THERMOCAPTCHA was deployed on the same server using our prototype implementation. For reCAPTCHA, we recorded the time from challenge appearance to verification; for THERMOCAPTCHA, we measured the time from thermal-image submission to the returned decision.

8.1 Participants and Procedure

We recruited 50 volunteers, including 20 visually challenged users. Participants came from multiple disciplines (including non-computer science fields), included both native and non-native English speakers, and comprised 12 women and 38 men. Each participant completed three THERMOCAPTCHA challenges and three reCAPTCHA

Table 9: Correct Attempt Ratio (CAR) and average completion time for THERMOCAPTCHA and reCAPTCHA. “W” = with glasses; “W/O” = without glasses.

CAPTCHA System	Normal Users		visually challenged Users			
	CAR (%)	Avg. Time (s)	W-CAR (%)	W-Time (s)	W/O-CAR (%)	W/O-Time (s)
THERMOCAPTCHA	94.70	6.56	96.77	6.75	95.23	7.36
reCAPTCHA	82.50	13.32	70.59	14.50	48.39	19.95

challenges, receiving pass/fail feedback for each attempt. Completion times and correctness outcomes were logged automatically.

Because thermal-image-based CAPTCHAs are unfamiliar to most users, we provided a brief instructional page explaining how to solve each challenge. The detailed questionnaire layout and instructions appear in Appendix F, and the full questionnaire text is provided in Appendix A. To promote inclusivity, the study followed WCAG accessibility principles [50], and an undergraduate assistant who was not involved in the design or implementation of THERMOCAPTCHA administered all sessions to reduce experimenter bias. On average, each participant spent 9.7 minutes completing the study.

In line with prior accessibility work and W3C reports, we used a short Likert-style questionnaire rather than the System Usability Scale (SUS) to better capture nuanced experiences of users with disabilities [18, 51]. The questionnaire focused on perceived comfort, fun, and ease of use of THERMOCAPTCHA relative to reCAPTCHA.

8.2 Completion Time and Accuracy

Table 9 summarizes the Correct Attempt Ratio (CAR) and average completion time for both systems. THERMOCAPTCHA exceeds the 90% usability benchmark suggested by Chellapilla et al. [16]. Among normal users, the 30 participants were required to complete 90 THERMOCAPTCHA challenges in total (three per participant). Five of these attempts failed on the first try and required retries, resulting in 95 total attempts to obtain 90 successful completions. This corresponds to a CAR of $90/95 = 94.70\%$. For reCAPTCHA, 90 intended challenges required 109 total attempts, with 90 successful completions and 19 failures, yielding a CAR of 82.50%.

For visually challenged participants, THERMOCAPTCHA similarly outperformed reCAPTCHA. With glasses, they achieved a CAR of 96.77% for THERMOCAPTCHA versus 70.59% for reCAPTCHA; without glasses, the CARs were 95.23% and 48.39%, respectively. Completion times followed the same trend: normal users completed THERMOCAPTCHA in an average of 6.56 s, compared to 13.32 s for reCAPTCHA. visually challenged users required 6.75–7.36 s for THERMOCAPTCHA and 14.50–19.95 s for reCAPTCHA.

As shown in Table 9, THERMOCAPTCHA achieves substantially faster completion times than reCAPTCHA across all user groups. Figure 9 (Appendix) provides the full distribution of completion times, confirming that the averages are representative and not driven by outliers. Notably, users unfamiliar with thermal images performed as well as those experienced with reCAPTCHA, underscoring the usability of THERMOCAPTCHA, particularly for visually challenged users.

8.3 Subjective Usability Perceptions

After completing all challenges, participants rated THERMOCAPTCHA and reCAPTCHA on fun, ease of use, and overall comfort using 5-point Likert scales. The majority of normal users (73.30%) and visually challenged users (60%) preferred THERMOCAPTCHA on fun and ease-of-use ratings (scores 4–5). Ease-of-use ratings were particularly strong: 86.67% of normal users and 75% of visually challenged users rated THERMOCAPTCHA as easier or much easier to use than reCAPTCHA.

Participants also reported higher comfort with THERMOCAPTCHA than with reCAPTCHA, frequently citing reduced visual strain and fewer repeated failures. When asked about adoption, all participants expressed interest in using THERMOCAPTCHA in practice, with normal users emphasizing convenience and ease of use and visually challenged users highlighting speed and reduced visual demand. Detailed distributions and plots for these subjective responses appear in Appendix F.

9 Discussion and Ethical Considerations

9.1 Limitations

Single-Class Detection Strategy. THERMOCAPTCHA employs a single-class detector trained primarily on human thermal images along with synthetically derived outliers. While this strategy is effective for distinguishing “human” versus “non-human” inputs, it does not provide fine-grained object categorization. The reported accuracy therefore reflects the model’s ability to detect deviations from the thermal patterns characteristic of humans rather than general-purpose recognition performance. Future work may explore multi-class thermal detection or contrastive learning techniques to improve generalization.

Limited Evaluation with Users Having Hearing Impairments. Because THERMOCAPTCHA requires no audio perception, we expect strong usability for individuals with hearing impairments. However, formal user studies with hearing-impaired participants required specialized institutional approval and could not be completed within our study window. The results from visually challenged participants—high Correct Attempt Ratios (CAR), short completion times, and strong subjective ratings—suggest promising accessibility potential. A dedicated accessibility study remains an important direction for follow-up work.

Availability of Thermal Hardware. Thermal cameras are not yet standard on consumer devices, which poses a deployment barrier. Nonetheless, inexpensive smartphone-compatible modules (as low as \$38) are increasingly common and widely used in professional applications [6]. THERMOCAPTCHA is designed to leverage such accessories when available, while falling back to a traditional CAPTCHA when thermal imaging is not supported. This hybrid design preserves inclusivity and avoids locking users out of protected services.

9.2 Security and Privacy Considerations

THERMOCAPTCHA strengthens defenses against automated attacks by combining thermal-based human verification with cryptographically bound, single-use traceable tokens. Unlike puzzle-based and behavioral CAPTCHAs—which are vulnerable to machine learning

solvers, mimicry attacks, and CAPTCHA-farm outsourcing—our design prevents token forwarding and enforces strong freshness and integrity guarantees. Furthermore, thermal images are inherently low-resolution and non-identifying; the system processes them in real time and discards them immediately, reducing privacy exposure. Because the CAPTCHA service is isolated from the relying website, cross-site profiling risks are minimized. Future enhancements include exploring differential privacy on metadata and evaluating deployment within trusted execution environments (TEEs).

9.3 Ethical Considerations

We implemented procedural and technical safeguards to ensure responsible use of thermal imaging. The research protocol—including dataset collection and usability testing—was reviewed and approved by the university Institutional Review Board (IRB). The study was classified as minimal risk, and data access was restricted to a small set of authorized researchers.

Thermal images collected during the study were processed directly by the model to compute variance metrics (Section 6). Volunteers received clear consent documentation outlining data handling, risks, and withdrawal rights. An independent undergraduate—uninvolved in system design—administered the user study to reduce experimenter bias.

For usability testing, both THERMOCAPTCHA and reCAPTCHA were presented in randomized order on a lab-hosted server. All participation occurred anonymously: Google Forms did not require login, sessions were conducted in Chrome’s incognito mode, and cookies were cleared between trials to avoid persistent camera permissions. Participants explicitly granted temporary thermal-camera access according to browser policy. These measures ensured transparency, privacy, and fair evaluation across all users.

10 Related Work

Thermal Imaging for Security and Privacy. Thermal cameras have been used in prior research to study unintended information leakage from user interactions. Abdelrahman et al. demonstrated that thermal residues left on touchscreens can allow adversaries to infer PINs and unlock patterns [11]. Subsequent work examined the persistence of thermal traces and factors influencing attack success [8, 21, 45]. These studies illustrate the sensitivity of thermal signals for reconstructing user actions. In contrast to these attack-focused applications, THERMOCAPTCHA leverages thermal imaging defensively: instead of extracting sensitive information, it relies on coarse heat distributions to verify human presence while preserving anonymity.

Facial Authentication and Liveness Detection. Modern smartphones frequently employ facial recognition systems [20, 32], though many still rely on 2D imagery, which is vulnerable to replay or print attacks. Farrukh et al. proposed FaceRevelio, a liveness-detection approach that reconstructs coarse 3D facial geometry using a single RGB camera illuminated by dynamic light patterns [19]. Similar techniques such as SciFi use randomized illumination patterns for stronger spoof resistance [54]. However, these methods depend heavily on controlled lighting and are sensitive to strong ambient light or occlusion. In contrast, THERMOCAPTCHA uses thermal

imaging, which is robust to illumination changes and focuses only on the presence of a heat-emitting human body rather than identity recognition.

Interaction-Based CAPTCHAs. Many traditional CAPTCHA schemes require explicit user interaction, such as clicking, dragging, or locating target regions. SACaptcha prompts users to identify specific shapes in an image [48], VAPTCHA requires tracing a randomly generated trajectory [28], and Ali et al. introduced a drag-and-drop puzzle CAPTCHA [13]. While these approaches can resist simple bots, they impose dexterity requirements and raise accessibility concerns for users with motor impairments or limited device precision. THERMOCAPTCHA removes these interaction burdens, requiring only a single capture event rather than manual input.

Cognitive and Behavioral CAPTCHAs. A number of recent systems employ cognitive challenges or behavioral biometrics. Gametrics uses mouse-movement patterns in a dynamic task [36]; Tencent, GEETest, and Netase deploy sliding-image CAPTCHAs requiring puzzle-piece alignment [56]; EYE-CAPTCHA relies on users solving mathematical tasks via eye movement tracking [47]; and Mantri et al. use motion-based interactions from accelerometer data [33]. Guerar et al. proposed an “Invisible” CAPTCHA that evaluates user behavior without explicit challenges [22]. However, many of these systems suffer from usability issues, particularly for older adults and users with cognitive or physical impairments. Moreover, Zhao et al. showed that sliding CAPTCHAs can be solved with up to 98% success using automated attacks [56].

THERMOCAPTCHA addresses these limitations by avoiding interaction-heavy or cognitively demanding tasks and by employing thermal features that are difficult to spoof while requiring minimal effort from the user.

11 Conclusion

This paper introduced THERMOCAPTCHA, a thermal-image-based human-verification mechanism that combines privacy-preserving sensing with cryptographically bound, single-use traceable tokens to counter CAPTCHA-farm forwarding. Our design addresses key limitations of existing CAPTCHA systems, which often impose cognitive or visual burdens and remain vulnerable to token reuse.

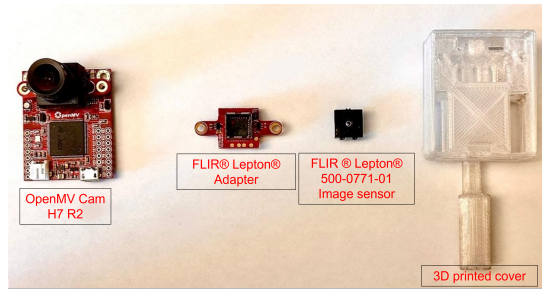
Our empirical evaluation shows that THERMOCAPTCHA achieves 96.70% human-detection accuracy with low verification latency, remains robust across realistic variations in angle, distance, and background conditions, and withstands MITM, spoofing, and adversarial attacks. A 50-participant usability study further demonstrates faster completion times and higher success rates than reCAPTCHA v2, particularly for visually challenged users.

While thermal sensors are not yet standard on consumer devices, their growing availability suggests a viable path toward broader adoption. Future work includes expanding cross-environment datasets, integrating differential privacy, and exploring deployment within trusted execution environments. Overall, THERMOCAPTCHA offers a promising direction for next-generation CAPTCHAs that balance usability, accessibility, and security.

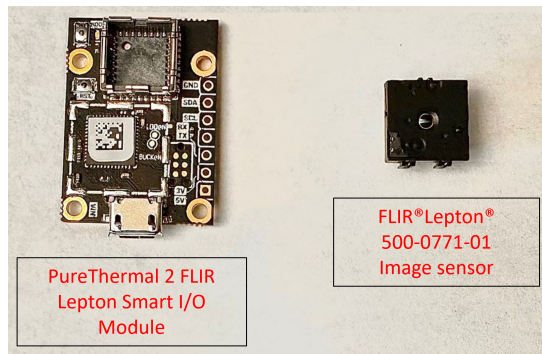
References

- [1] [n. d.]. 9kw.eu - Captcha Service for the user - captcha solver. <https://www.9kw.eu/>. (Accessed on 07/10/2024).
- [2] [n. d.]. Accessibility at hCaptcha: Current and Future Plans | Blog - hCaptcha. <https://www.hcaptcha.com/post/accessibility-at-hcaptcha-current-and-future-plans>. (Accessed on 05/18/2022).
- [3] [n. d.]. GitHub - AlexeyAB/darknet: YOLOv4 / Scaled-YOLOv4 / YOLO - Neural Networks for Object Detection (Windows and Linux version of Darknet). <https://github.com/AlexeyAB/darknet>. (Accessed on 07/09/2024).
- [4] [n. d.]. Google Online Security Blog: reCAPTCHA just got easier (but only if you're human). https://web.archive.org/web/20160308094521mp_/https://googleonlinesecurity.blogspot.com/2013/10/recaptcha-just-got-easier-but-only-if.html. (Accessed on 07/05/2024).
- [5] [n. d.]. Loading reCAPTCHA | Google for Developers. <https://developers.google.com/recaptcha/docs/loading>. (Accessed on 07/05/2024).
- [6] [n. d.]. Mobile Thermal Imager 32*32 Pixels -20-1000°C Thermal Camera Thermal Imaging Camera for Android Type C Phones Infrared Camera - AliExpress. <https://www.aliexpress.us/item/3256806845123504.html?src=google&gatewayAdapt=glo2usa>. (Accessed on 10/23/2024).
- [7] [n. d.]. ReCAP: A distributed CAPTCHA service at the edge of the network to handle server overload - Al-Hammouri - 2018 - Transactions on Emerging Telecommunications Technologies - Wiley Online Library. <https://onlinelibrary.wiley.com/doi/abs/10.1002/ett.3187>. (Accessed on 07/10/2024).
- [8] [n. d.]. Research & Development | Teledyne FLIR. <https://www.flir.com/applications/science/>. (Accessed on 10/08/2022).
- [9] 2Captcha. 2024. Captcha Solver: Captcha solving service includes reCAPTCHA solver and any captchas auto solver. Bypass captchas using the best captcha solver online API - 2Captcha. <https://2captcha.com/>. (Accessed on 07/10/2024).
- [10] R Aadhirai, P J Sathish Kumar, and S Vishnupriya. 2012. Image CAPTCHA: Based on human understanding of real world distances. In *2012 4th International Conference on Intelligent Human Computer Interaction (IHCI)*. IEEE, 1–6.
- [11] Yomna Abdelrahman, Mohamed Khamis, Stefan Schneegass, and Florian Alt. 2017. Stay cool! understanding thermal attacks on mobile-based user authentication. In *Proceedings of the 2017 CHI Conference on Human Factors in Computing Systems*. 3751–3763.
- [12] Ako Muhamad Abdullah et al. 2017. Advanced encryption standard (AES) algorithm to encrypt and decrypt data. *Cryptography and Network Security* 16, 1 (2017), 11.
- [13] Firkhan Ali Bin Hamid Ali and Farhana Bt Karim. 2014. Development of CAPTCHA system based on puzzle. In *2014 International Conference on Computer, Communications, and Control Technology (I4CT)*. IEEE, 426–428.
- [14] anti captcha. 2020. Solve Google Recaptcha automatically. <https://anti-captcha.com/apidoc/task-types/RecaptchaV2Task> [Online; accessed 2025-04-23].
- [15] Mrinal Kanti Bhowmik, Kankan Saha, Sharmistha Majumder, Goutam Majumder, Ashim Saha, A Nath Sarma, Debotosh Bhattacharjee, Dipak Kumar Basu, and Mita Nasipuri. 2011. Thermal infrared face recognition—a biometric identification technique for robust security system. *Reviews, refinements and new ideas in face recognition* 7 (2011), 113–138.
- [16] Kumar Chellapilla, Kevin Larson, Patrice Y Simard, and Mary Czerwinski. 2005. Building segmentation based human-friendly human interaction proofs (HIPs). In *Human Interactive Proofs: Second International Workshop, HIP 2005, Bethlehem, PA, USA, May 19-20, 2005. Proceedings*. Springer, 1–26.
- [17] deathbycaptcha. 2020. API New Token Recaptcha | Death By Captcha | en. <https://deathbycaptcha.com/api/newtokenrecaptcha> [Online; accessed 2025-04-23].
- [18] Valerie Fanelle, Sepideh Karimi, Aditi Shah, Bharath Subramanian, and Sauvvik Das. 2020. Blind and human: Exploring more usable audio {CAPTCHA} designs. In *Sixteenth Symposium on Usable Privacy and Security (SOUPS 2020)*. 111–125.
- [19] Habiba Farukh, Reham Mohamed Aburas, Siyuan Cao, and He Wang. 2020. FaceRevelio: a face liveness detection system for smartphones with a single front camera. In *Proceedings of the 26th Annual International Conference on Mobile Computing and Networking*. 1–13.
- [20] Mohammed E Fathy, Vishal M Patel, and Rama Chellappa. 2015. Face-based active authentication on mobile devices. In *2015 IEEE international conference on acoustics, speech and signal processing (ICASSP)*. IEEE, 1687–1691.
- [21] Anjith George, Zohreh Mostaani, David Geissenbuhler, Olegs Nikisins, André Anjos, and Sébastien Marcel. 2019. Biometric face presentation attack detection with multi-channel convolutional neural network. *IEEE Transactions on Information Forensics and Security* 15 (2019), 42–55.
- [22] Meriem Guerar, Alessio Merlo, Mauro Migliardi, and Francesco Palmieri. 2018. Invisible CAPPCHA: A usable mechanism to distinguish between malware and humans on the mobile IoT. *computers & security* 78 (2018), 255–266.
- [23] Meriem Guerar, Luca Verderame, Mauro Migliardi, Francesco Palmieri, and Alessio Merlo. 2021. Gotta CAPTCHA'Em all: a survey of 20 Years of the human-or-computer Dilemma. *ACM Computing Surveys (CSUR)* 54, 9 (2021), 1–33.
- [24] Carlos Javier Hernández-Castro, David F Barrero, Shujun Li, et al. 2017. An oracle-based attack on CAPTCHAs protected against oracle attacks. *arXiv preprint arXiv:1702.03815* (2017).
- [25] Carlos Javier Hernandez-Castro and Arturo Ribagorda. 2010. Pitfalls in CAPTCHA design and implementation: The Math CAPTCHA, a case study. *computers & security* 29, 1 (2010), 141–157.
- [26] Md Imran Hossen, Yazhou Tu, Md Fazle Rabby, Md Nazmul Islam, Hui Cao, and Xiali Hei. 2020. An object detection based solver for google's image recaptcha v2. In *23rd International Symposium on Research in Attacks, Intrusions and Defenses (RAID 2020)*.
- [27] Yasha Irvantchi, Thomas Krolikowski, William Wang, Kang G Shin, and Alanson Sample. 2024. PrivacyLens: On-Device PII Removal from RGB Images using Thermally-Enhanced Sensing. *Proceedings on Privacy Enhancing Technologies YYYY (X) 1* (2024), 20.
- [28] YUAN Jingxia. 2020. Variation analysis-based public turing test to tell computers and humans apart. US Patent 10,657,243.
- [29] kolotibablo. 2027. Captcha Solving Job. <https://kolotibablo.com/> [Online; accessed 2025-04-23].
- [30] Adrian Kristanto, Maxime Cordeil, Benjamin Tag, Nathalie Henry Riche, and Tim Dwyer. 2023. Hanstreamer: an Open-source Webcam-based Live Data Presentation System. *arXiv preprint arXiv:2309.12538* (2023).
- [31] Shinfeng D Lin, Luming Chen, and Wensheng Chen. 2021. Thermal face recognition under different conditions. *BMC bioinformatics* 22 (2021), 1–17.
- [32] Upal Mahbub, Vishal M Patel, Deepak Chandra, Brandon Barbello, and Rama Chellappa. 2016. Partial face detection for continuous authentication. In *2016 IEEE international conference on Image processing (ICIP)*. IEEE, 2991–2995.
- [33] Viraj C Mantri and Prateek Mehrotra. 2018. User authentication based on physical movement information. US Patent 9,864,854.
- [34] Ralph C Merkle. 1987. A digital signature based on a conventional encryption function. In *Conference on the theory and application of cryptographic techniques*. Springer, 369–378.
- [35] mitproxy. 2024. mitproxy - an interactive HTTPS proxy. <https://mitproxy.org/>. (Accessed on 07/09/2024).
- [36] Manar Mohamed and Nitesh Saxena. 2016. Gametrics: towards attack-resilient behavioral authentication with simple cognitive games. In *Proceedings of the 32nd Annual Conference on Computer Security Applications*. 277–288.
- [37] Marti Motoyama, Kirill Levchenko, Chris Kanich, Damon McCoy, Geoffrey M Voelker, and Stefan Savage. 2010. Re: {CAPTCHAs—Understanding} {CAPTCHA-Solving} services in an economic context. In *19th USENIX Security Symposium (USENIX Security 10)*.
- [38] Ananya Narayanawamy. 2022. CAPTCHAs in reality: What might happen if they are easily broken? *Journal of Student Research* 11, 3 (2022).
- [39] Hoang Dai Nguyen, Karthika Subramani, Bhupendra Acharya, Roberto Perdisci, and Phani Vadrevu. 2024. C-FRAME: Characterizing and measuring in-the-wild CAPTCHA attacks. (2024).
- [40] Onn Nir. 2023. reCAPTCHA Privacy – Is it an Oxymoron Now? – Reflectiz. <https://www.reflectiz.com/blog/recaptcha-privacy/>. (Accessed on 07/10/2024).
- [41] reCAPTCHA. 2022. reCAPTCHA v2 - Solve reCAPTCHA v2 API | 2Captcha - captcha bypass service. <https://2captcha.com/api-docs/recaptcha-v2> [Online; accessed 2025-04-23].
- [42] reCAPTCHA. 2024. reCAPTCHA. <https://www.google.com/recaptcha/about/>. (Accessed on 05/18/2022).
- [43] Alia Saad, Kian Izadi, Anam Ahmad Khan, Pascal Knierim, Stefan Schneegass, Florian Alt, and Yomna Abdelrahman. 2023. HotFoot: Foot-Based User Identification Using Thermal Imaging. In *Proceedings of the 2023 CHI Conference on Human Factors in Computing Systems*. 1–13.
- [44] Andrew Searles, Yoshimichi Nakatsuka, Ercan Ozturk, Andrew Paverd, Gene Tsudik, and Ai Enkoji. 2023. An Empirical Study & Evaluation of Modern {CAPTCHAs}. In *32nd usenix security symposium (usenix security 23)*. 3081–3097.
- [45] Fatih Mehmet Senalp and Murat Ceylan. 2022. Effects of the deep learning-based super-resolution method on thermal image classification applications. *Multimedia Tools and Applications* 81, 7 (2022), 9313–9330.
- [46] Connor Shorten and Taghi M Khoshgofaar. 2019. A survey on image data augmentation for deep learning. *Journal of big data* 6, 1 (2019), 1–48.
- [47] Apichai Siripitakchai, Suphakant Phimoltares, and Atchara Mahaweerawat. 2017. EYE-CAPTCHA: An enhanced CAPTCHA using eye movement. In *2017 3rd IEEE International Conference on Computer and Communications (ICCC)*. IEEE, 2120–2126.
- [48] Mengyun Tang, Haichang Gao, Yang Zhang, Yi Liu, Ping Zhang, and Ping Wang. 2018. Research on deep learning techniques in breaking text-based captchas and designing image-based captcha. *IEEE Transactions on Information Forensics and Security* 13, 10 (2018), 2522–2537.
- [49] Luis Von Ahn, Manuel Blum, and John Langford. 2004. Telling humans and computers apart automatically. *Commun. ACM* 47, 2 (2004), 56–60.
- [50] w3. 2020. Web Content Accessibility Guidelines (WCAG) 2.0. <https://www.w3.org/TR/WCAG20/>. (Accessed on 07/10/2024).
- [51] w3. 2021. Inaccessibility of CAPTCHA. <https://www.w3.org/TR/turingtest/#the-accessibility-challenge>. (Accessed on 10/20/2024).

- [52] Ping Wang, Haichang Gao, Xiaoyan Guo, Chenxuan Xiao, Fuqi Qi, and Zheng Yan. 2023. An Experimental Investigation of Text-based CAPTCHA Attacks and Their Robustness. *Comput. Surveys* 55, 9 (2023), 1–38.
- [53] Benedikt Wolters. 2022. Announcing Turnstile, a user-friendly, privacy-preserving alternative to CAPTCHA. <https://blog.cloudflare.com/turnstile-private-captcha-alternative/>. (Accessed on 07/05/2024).
- [54] Wuyuan Xie, Zhaonian Kuang, and Miaohui Wang. 2021. SCIFI: 3D face reconstruction via smartphone screen lighting. *Optics Express* 29, 26 (2021), 43938–43952.
- [55] Zhao Zhang, Tavish Vaidya, Kartik Subramanian, Wenchao Zhou, and Micah Sherr. 2020. Ephemeral exit bridges for tor. In *2020 50th Annual IEEE/IFIP International Conference on Dependable Systems and Networks (DSN)*. IEEE, 253–265.
- [56] Binbin Zhao, Haiqin Weng, Shouling Ji, Jianhai Chen, Ting Wang, Qinming He, and Reheem Beyah. 2018. Towards evaluating the security of real-world deployed image captchas. In *Proceedings of the 11th ACM Workshop on Artificial Intelligence and Security*. 85–96.



(a) Module for dataset collection



(b) Module for real-time webcam capture

Figure 7: Thermal imaging modules used in our study.

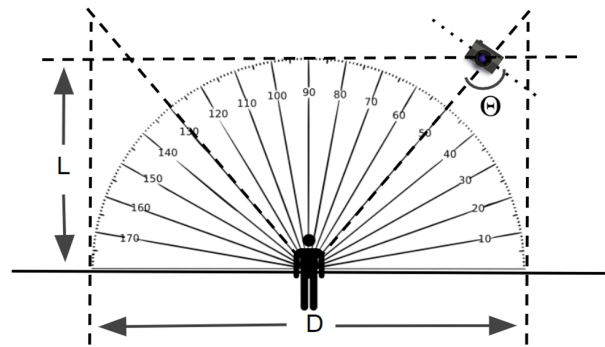
A Data Availability

To support replication, we provide all artefacts necessary to reproduce our system, training pipeline, and usability study, subject to the constraints of our Institutional Review Board (IRB) protocol. The IRB requires that access to raw thermal-image data be restricted to researchers who have completed appropriate human-subjects training. Accordingly, the thermal dataset will be made available upon request to individuals who provide proof of such training (e.g., CITI certification), consistent with the approved data-handling procedures. An anonymous GitHub repository⁶ contains the following artefacts:

- detailed training instructions, configuration files, and augmentation scripts,



(a) Physical data-collection setup



(b) Schematic diagram of the setup

Figure 8: Data-collection environment. In (b), D is the circle diameter defining subject positions, L is the camera–subject distance, and Θ is the viewing angle.

- pre-trained YOLOv4-tiny model weights used in our evaluation,
- the complete ThermoCAPTCHA implementation (client widget, server backend, and database schema),
- and the usability-study questionnaire referenced in Section 8.

These artefacts enable end-to-end reproduction of the training pipeline, system deployment, and usability evaluation. Researchers requesting access to the raw thermal dataset will receive it after meeting the IRB-mandated training requirements.

B Data Collection Setup

Figures 7(a) and 7(b) show the two thermal-camera modules used in our experiments. The first module was used to collect the dataset and train the model; the second served as a plug-and-play USB thermal webcam for real-time CAPTCHA verification.

The physical recording environment is shown in Figure 8(a), and its corresponding geometric layout appears in Figure 8(b). As indicated in the diagram, D represents the circular arc diameter along which subjects rotated to vary horizontal viewing angle, L is the fixed camera–subject distance, and Θ is the angle subtended at the

⁶Anonymous replication package: <https://github.com/anonymouspaul96/Live-Thermal-Image-based-CAPTCHA>.

Table 10: Comparison of YOLOv4-tiny checkpoints saved every 10,000 iterations.

Weights	Detections Count	Unique Count	Conf. Thresh.	TP	FP	FN	Prec. (%)	Recall (%)	F1 (%)	IoU (%)	Avg. IoU (%)	mAP (%)
10,000	1,286	745	0.25	722	257	23	74.0	97.0	84.0	50	59.14	80.89
20,000	2,343	745	0.25	716	319	29	69.0	96.0	80.0	50	53.77	78.53
30,000	2,756	745	0.25	715	212	30	77.0	96.0	86.0	50	61.51	83.55
40,000	3,695	745	0.25	695	529	50	57.0	93.0	71.0	50	44.88	74.82

camera. These figures document the controlled capture conditions employed during dataset creation.

C Dataset and Weight Analysis

This section provides supporting details on the construction of the thermal dataset used for model training and evaluation, as well as an analysis of the YOLOv4-tiny weight checkpoints generated during the training process. The main paper reports aggregate results; here we include full dataset composition and per-weight performance metrics for transparency and replicability.

C.1 Dataset

A total of 286 thermal images were collected from 26 participants, each contributing 11 images under controlled pose and angle conditions. Of these, 110 images were allocated to the test set, and an additional 10 images of non-human thermal objects (e.g., hot containers, appliances) were reserved for robustness evaluations. The remaining 176 images were used for model training.

To expand the training corpus, we applied standard geometric and photometric augmentations, generating 20 variants per image and producing 3,520 augmented samples in total. All training, testing, and evaluation images were mutually disjoint to avoid data leakage.

C.2 Weight Analysis

The YOLOv4-tiny model was trained for 40,000 iterations on an Ubuntu 20.04 system. Training converged to an average loss of 0.0509. We evaluated snapshot weight files saved at 10,000 iteration intervals to identify the checkpoint with the best performance.

Table 10 compares key metrics—precision, recall, F1-score, IoU, and mean average precision (mAP)—across checkpoints. The 30,000-iteration checkpoint (‘yolov4-custom_30000.weights’) achieved the highest mAP (83.55%) and the best overall balance between precision and recall, and was therefore selected as the deployed detector for ThermoCAPTCHA.

D Detailed FGSM Evaluation Results

This section expands on the adversarial robustness results summarized in Section 7.2. We evaluated FGSM perturbations across seven distortion budgets using 20 thermal samples (10 human, 10 non-human). For each ϵ , we report (i) evasion (human \rightarrow non-human), (ii) induction (non-human \rightarrow human), and (iii) overall misclassification rate. To illustrate the qualitative nature of these perturbations, Table 11 presents adversarial examples from a representative thermal sample.

Table 12 shows the quantitative misclassification outcomes across all 20 samples. Perturbations with $\epsilon \leq 0.10$ produced no misclassifications, while substantial degradation occurred only at large distortion budgets ($\epsilon \geq 0.30$) that introduce visually unrealistic artifacts.

E Proof of Token Reuse Infeasibility

We formally show that a traceable token issued by the ThermoCAPTCHA cannot be reused by an attacker, even when a legitimate CAPTCHA-farm worker W forwards the exact ciphertext to an adversary A . The security argument relies on the binding of the token to session- and device-specific values and on the unforgeability of the MAC under the shared secret key.

Notation. Let:

- T : the traceable token,
- SK_{server} : CAPTCHA server secret key (used for encryption),
- K_{shared} : shared secret between the web server and CAPTCHA service,
- $sess_{id}$: session identifier,
- dev_{fp} : device fingerprint,
- $nonce$: freshness nonce,
- exp : expiration timestamp,
- UID : user identifier (e.g., IP, public-key hash).

Token Construction. The server constructs a token of the form:

$$T = \text{Enc}_{SK_{\text{server}}} \left(\text{MAC}_{K_{\text{shared}}} (UID \parallel sess_{id} \parallel dev_{fp} \parallel nonce \parallel exp) \right). \quad (1)$$

Attack Scenario. Assume a worker W legitimately solves a CAPTCHA and receives:

$$T_W = \text{Enc}_{SK_{\text{server}}} \left(\text{MAC}_{K_{\text{shared}}} (UID_W \parallel sess_{id}^W \parallel dev_{fp}^W \parallel nonce^W \parallel exp^W) \right). \quad (2)$$

The worker forwards T_W to an attacker A , who issues a verification request from a different device, session, and network context. The CAPTCHA server decrypts T_W and recomputes the MAC on:

$$\text{MAC}_{K_{\text{shared}}} (UID_A \parallel sess_{id}^A \parallel dev_{fp}^A \parallel nonce^W \parallel exp^W). \quad (3)$$

Mismatch of Context-Bound Values. Forwarding necessarily changes at least one of:

$$(UID, sess_{id}, dev_{fp}),$$

so we have:

$$(UID_A, sess_{id}^A, dev_{fp}^A) \neq (UID_W, sess_{id}^W, dev_{fp}^W).$$

Table 11: Representative FGSM adversarial examples across different ϵ values. Each column shows the perturbed thermal image (top), perturbation pattern (middle), and the corresponding difference map (bottom). Confidence values refer to the human-detection score output by the model.

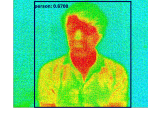
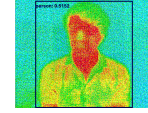
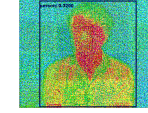
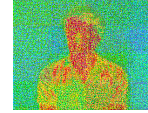
ϵ	0.01	0.02	0.03	0.10	0.20	0.30	0.50
Adversarial Image	 Conf: 0.9283	 Conf: 0.8978	 Conf: 0.8312	 Conf: 0.7590	 Conf: 0.6700	 Conf: 0.5152	 Conf: 0.3200
Perturbation Pattern							
Difference Map							

Table 12: FGSM misclassification rates across 20 thermal samples.

ϵ	Evasion	Induction	Success (%)	Miscls.
0.01	0%	0%	0%	0/20
0.02	0%	0%	0%	0/20
0.03	0%	0%	0%	0/20
0.10	0%	0%	0%	0/20
0.20	10%	0%	5%	1/20
0.30	40%	20%	30%	6/20
0.50	90%	70%	80%	16/20

Failure of MAC Verification. From the unforgeability of MACs under K_{shared} , it follows that:

$$\text{MAC}_{K_{\text{shared}}}(A) \neq \text{MAC}_{K_{\text{shared}}}(W),$$

so verification of T_W in attacker context A always fails.

Conclusion. The token T_W cannot be validated outside the original execution context. Thus, the probability that attacker A successfully reuses a forwarded token is:

$$\Pr[\text{Reuse of token } T_W \text{ by attacker } A] = 0,$$

under standard assumptions on the security of the encryption and MAC primitives.

F User Study Methodology and Usability Statistics

This appendix provides additional methodological details and extended usability statistics for the comparative study between THERMOCAPTCHA and Google reCAPTCHA described in Section 8. The main text summarizes the participant population, core procedure,

and key quantitative results; here we expand on (i) the study protocol and ethical safeguards, and (ii) detailed subjective usability outcomes.

F.1 Additional Methodological Details

As noted in Section 8, each participant solved three THERMOCAPTCHA challenges and three reCAPTCHA challenges. Both systems were deployed on the lab website and accessed via Google Forms. The order of THERMOCAPTCHA and reCAPTCHA challenges was randomized to reduce ordering effects.

To maintain ethical standards, each participant was presented with three documents before participation:

- a CITI Program certificate verifying that the research team completed Human Subjects Research training,
- a flyer explaining the study goals and overall procedure, and
- an informed-consent form describing risks, data handling practices, and the right to withdraw at any time.

The study took place in a controlled lab environment and was overseen by an undergraduate surveyor who was not involved in the design or implementation of THERMOCAPTCHA, in order to minimize experimenter bias. Participants completed the tasks using Google Chrome in incognito mode, and the Google Form did not require login, preserving anonymity.

When solving THERMOCAPTCHA, participants were prompted by the browser to grant camera access. Because some browsers cache camera permissions across page loads, cookies and site data were cleared between sessions to ensure a consistent permission workflow for all users. Both interfaces followed Web Content Accessibility Guidelines (WCAG) [50].

The questionnaire layout (referenced in Section 8) consisted of:

- an initial one-page guide explaining how to solve each challenge in THERMOCAPTCHA and reCAPTCHA,
- three distinct THERMOCAPTCHA challenges,

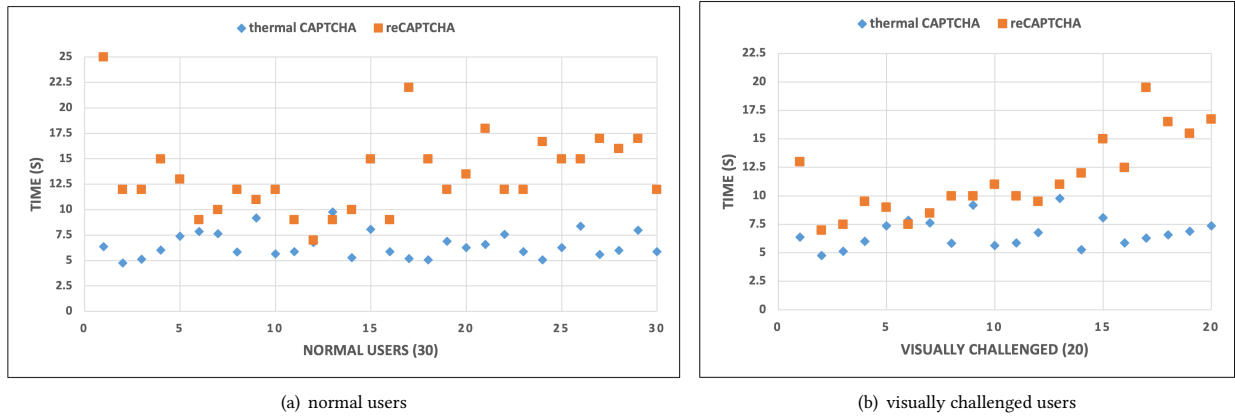


Figure 9: Timing distribution of THERMOCAPTCHA and reCAPTCHA for sighted and visually challenged users.

- three distinct reCAPTCHA challenges,
- a short questionnaire on familiarity with CAPTCHAs and experience with face-authentication systems (e.g., blinking, smiling, liveness checks), and
- a final questionnaire asking users to rate THERMOCAPTCHA on comfort, fun, and ease of use relative to reCAPTCHA.

For subjective evaluation, we used Likert-style questions rather than the System Usability Scale (SUS), following W3C accessibility recommendations and prior work on blind and visually challenged users [18, 51]. Participants rated THERMOCAPTCHA and reCAPTCHA on fun and ease of use using a 5-point scale:

- 1-2: reCAPTCHA is more fun/easy,
- 3: both systems are equally fun/easy,
- 4-5: THERMOCAPTCHA is more fun/easy.

Separate 1-5 scales were used for overall comfort and for willingness to adopt THERMOCAPTCHA in real deployments.

F.2 Extended Usability Statistics

Table 9 in the main text reports the Correct Attempt Ratio (CAR) and completion times across user groups and conditions. Here we provide additional subjective statistics that complement those quantitative results.

After completing all six challenges, participants rated fun and ease of use for both systems. Figure 10 breaks down these responses by user group.

For normal users, 73.30% of responses fell in the 4-5 range, indicating that participants generally found THERMOCAPTCHA at least somewhat more fun and easier to use than reCAPTCHA. Among visually challenged users, 60% of responses were in the 4-5 range, with relatively few ratings in the 1-2 (reCAPTCHA-preferred) region. These distributions align with the summary statistics in Section 8, where 86.67% of sighted users and 75% of visually challenged users rated THERMOCAPTCHA as easier than or superior to reCAPTCHA.

We also collected detailed comfort ratings and self-reported reasons for preferring (or not preferring) THERMOCAPTCHA. Figure 11 shows the comfort distribution and the primary reasons cited.

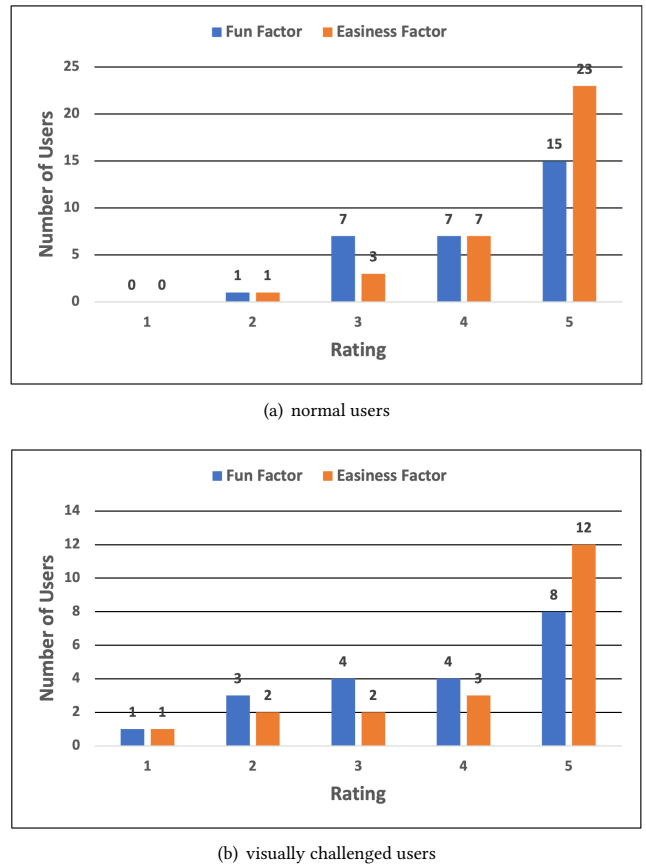
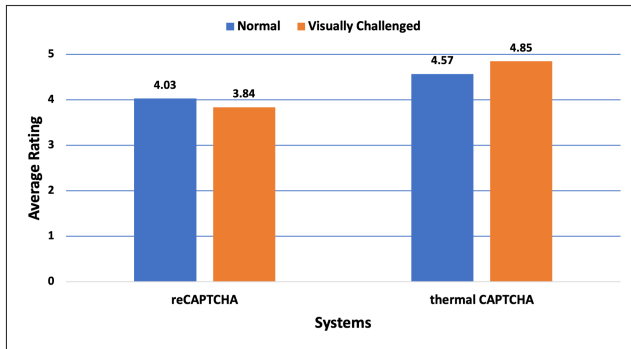
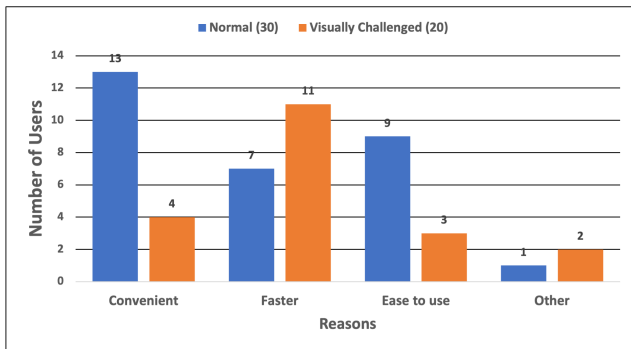


Figure 10: Fun and ease-of-use ratings for THERMOCAPTCHA vs. reCAPTCHA. Ratings 1-2 indicate a preference for reCAPTCHA, 3 indicates no preference, and 4-5 indicate a preference for THERMOCAPTCHA.



(a) Comfort levels



(b) Self-reported reasons

Figure 11: User comfort levels and self-reported reasons for preferring THERMOCAPTCHA over reCAPTCHA.

Both sighted and visually challenged users reported higher comfort with THERMOCAPTCHA than with reCAPTCHA. Among normal users, 43% selected convenience as their primary reason for preferring THERMOCAPTCHA, and 30% highlighted ease of use. Among visually challenged users, 55% cited speed as the dominant factor, with additional responses emphasizing reduced visual demand and lower frustration. These subjective results are consistent with the objective CAR and timing improvements reported in the main text, and together they support the conclusion that THERMOCAPTCHA offers both improved task performance and favorable user experience, particularly for users with visual impairments.